THE PRIMARY COSMIC RAY ELECTRON SPECTRUM FROM 10 GeV TO ABOUT 200 GeV

R. F. Silverberg*, J.F. Ormes, V.K. Balasubrahmanyan,
M. J. Ryan+
Goddard Space Flight Center,
Greenbelt, Md.

Abstract

An ionization spectrometer consisting of 10.8 radiation lengths of tungsten and 35 radiation lengths of iron has been used to determine the energy spectrum of cosmic ray electrons above 10 GeV. The spectrometer was calibrated with electrons from 5.4 to 18 GeV at the Stanford Linear Accelerator and then flown at an altitude of 6 gm-cm^{-2} for 16 hours. Separation of electron initiated events from proton events was achieved by utilizing starting point distributions, the shower development in tungsten, and the energy deposited in the large thickness of iron absorber. The exponent of the differential energy spectrum of the electrons is -3.1 ± 0.2 while the exponent of the background is consistent with the proton exponent of $-2.7 \pm .2$.

1. Introduction

The energy spectrum of cosmic ray electrons has been given much attention in recent years because of its astrophysical significance. While results up to a few hundred GeV have been obtained in balloon flights (Nishimura et al. 1969; Anand et al. 1968; Anand et al. 1969; Scheepmaker, 1971) serious discrepancies in the spectral shape and absolute intensity are apparent.

In the hope of clarifying the high energy electron spectrum, a large area electron detector was flown from Alamogordo, New Mexico in April of 1969 at a depth of 7.9 g/cm^2 residual atmosphere and again in November 1970 at 6.0 g/cm^2 for a total exposure factor of 4800 M^2-ster-sec.

2. Description of the Detector

The experiment consists of three main sections. These are: (a) the charge module consisting of three scintillators and a Cerenkov counter. A digitized spark chamber is used to determine the trajectory of particles so that geometrical corrections can be made to the pulse heights from the detectors. The spark chamber is also useful in eliminating particles entering the sides of the detector and other background; (b) the electron cascade section of the detector consists of 12 modules each containing a 1/8" thick tungsten sheet and a 1/4" plastic scintillator. Each module is 0.9 radiation lengths thick; (c) the nuclear cascade section consists of 7 iron modules each of which is 4.5 radiation lengths thick. (Its primary use is for nucleons; see Ryan et al. this conference.) This section of the detector was not flown on the 1969 flight.

A diagram of the experiment as flown in 1970 is shown in Figure 1.

*University of Maryland
+NAS-NRC Research Associate

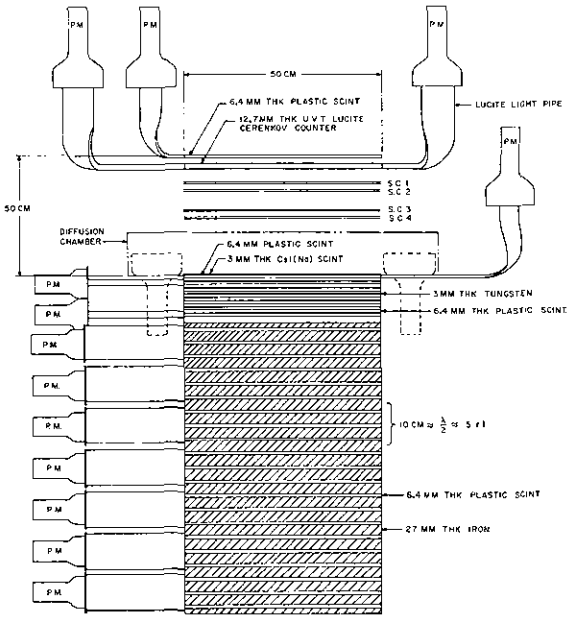

IONIZATION SPECTROMETER

3. Triggering Modes of the Experiment

In order to reduce background and the dead time in the experiment, the electron trigger criteria were set to demand the equivalent of a 7 GeV electron in the tungsten modules by requiring a minimum pulse height in each of the 12 scintillators. This not only discrminated against low energy particles, but also eliminated triggers from most of the high energy protons interacting deep in the tungsten. The only protons which triggered the electron mode were those which interacted early in the tungsten stack. In the proton trigger mode, particles were selected which deposited 40 GeV or more in the iron modules. These particles were used to determine the background proton correction to the electron intensity.

4. Energy Determination

The detector was calibrated on positrons from 5.4 to 18 GeV at the Stanford Linear Accelerator (SLAC) in 1969, and on protons up to 18 GeV at the Brookhaven National Laboratory in 1970.

The energy of an incident electron is determined by the minimization of the parameter $\chi^2 = \sum_i \frac{(N(E_o, t_o, t_i) - N_{\text{observed}}(t_i))^2}{\sigma^2(E_o, t_o, t_i)}$ (1)

where $N(E_o, t_o, t_i)$ is the number of particles that an electromagnetic cascade initiated by an electron of energy E_o will produce at depth t_i if it started to cascade at depth t_o. $\sigma^2(E_o, t_o, t_i)$ is the variance of $N(E_o, t_o, t_i)$. At SLAC energies, we observed $\sigma^2(E_o, t_o, t_i) \approx 4\, N(E_o, t_o, t_i)$ except at small depths where the deviations were larger.

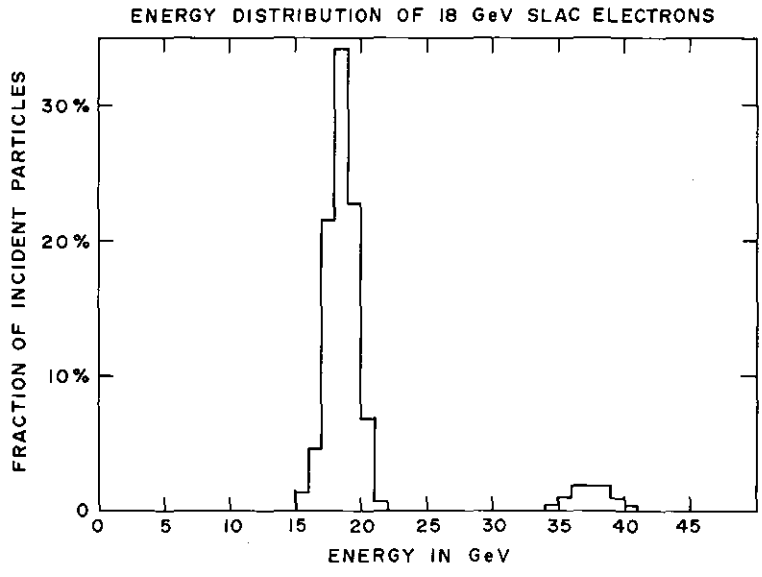

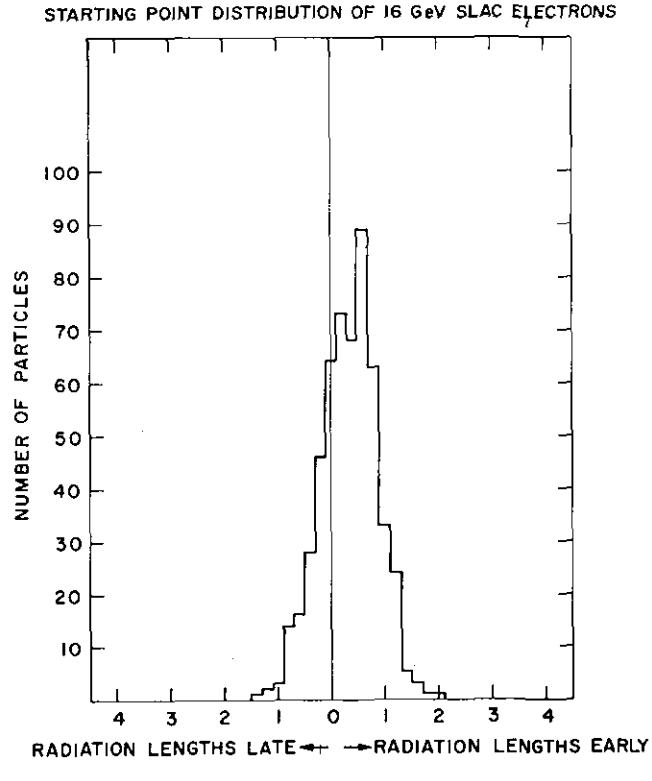

A two parameter fit to the data (E_o and t_o) is used to minimize χ^2. This determines E_o, the best estimate to the energy of the electron and t_o, the best estimate of its starting point. By using our data from SLAC, a χ^2 distribution for electrons was determined.

The energy distribution observed by applying the procedure outlined above to a run with 18 GeV electrons from SLAC is shown in Figure 2. The FWHM of the distribution is ~ 17%. The small peak below 40 GeV is due to two 18 GeV electrons incident on the experiment within the resolving time.

5. Discrimination against Protons

Due to the fact that the electron component of cosmic rays is at best only a few percent of the proton component, any measurement of electrons is usually plagued with a large component of protons which may masquerade as electrons. Any interaction which produces a π° meson may produce a cascade that is, in practice, indistinguishable from a cascade produced by an electron.

Our study of accelerator electrons and in-flight high energy protons has revealed that the method of fitting the cascades to the equation described above provides a sensitive means

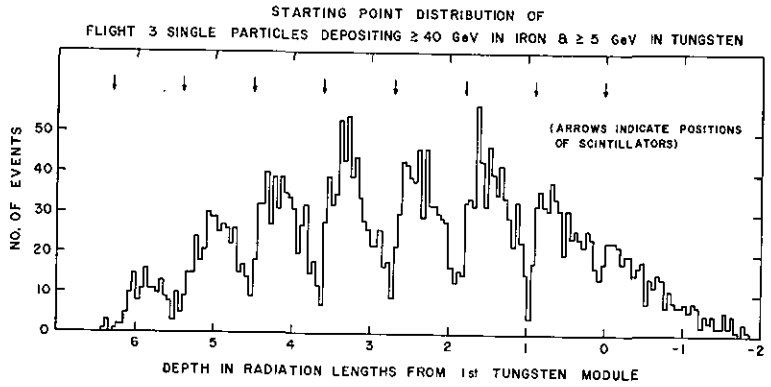

of discrimination against the proton background. In Figure 3 is presented the distribution of "apparent starting points" of a sample of 16 GeV electrons at SLAC. This curve is representative as we have noted no energy dependence from 5.4 to 18 GeV. Note that although there is only about 0.2 radiation lengths of material before the tungsten stack (0 radiation lengths on the graph), the "apparent starting point" distribution peaks at about 0.5 radiation lengths. In contrast to the electrons, a group of singly charged particles was selected from the 1970 flight which deposited $\geq$ 40 GeV in the iron and $\geq$ 5 GeV in the tungsten. Furthermore E (iron)/E (tungsten) > 1, implying that this class of particles is dominated by protons. Their "apparent starting point" distribution is shown in Figure 4.

The distribution in figure 4 exhibits marked structure. The source of the structure is not well understood at this time. One quarter of the interactions take place in the plastic scintillators which are invisible on this radiation length scale. The structure is the result of a competition between the process of fitting electromagnetic shower curves to nuclear interactions, the transport of γ-rays from π^0 decay into subsequent tungsten slabs and the shift of the "apparent starting point" by a few tenths of a radiation length. At any rate, the structure is real, is present for both protons and especially for background events and says that the shower fitting procedure is defining an "apparent starting point" with an accuracy of at least $\pm$.2 radiation lengths.

6. Data Analysis

Each possible electron event is examined to be sure that it is caused by a singly charged particle as determined by the top plastic scintillator and the Cerenkov detector. Both of these detectors are 30 cm above the tungsten stack. If the particle is singly charged, the spark chamber data is used to extrapolate the path of the particle to the twelfth tungsten module. Only particles whose trajectories pass inside of one inch of the edge of the 12th tungsten module are

analyzed.

Each possible electron event is then fitted to determine its energy and apparent starting point. The value of the minimum χ^2 is examined to see if the probability of it being an electron is greater than .05. If the apparent starting point is outside the limits observed at SLAC, the particle is discarded as it is likely to be caused by a proton interaction. Particles passing all of the above tests are estimated to be 85% electrons, the remaining 15% being background that is indistinguishable from electrons. It is important to note that the spectral index of rejected particles is -2.7 in agreement with the proton spectrum. We have also looked for energy dependent effects such as backscatter and find no effect large enough to cause the observed 0.5 change in spectral index. The resultant electron spectrum at the top of the atmosphere is presented in Figure 5.

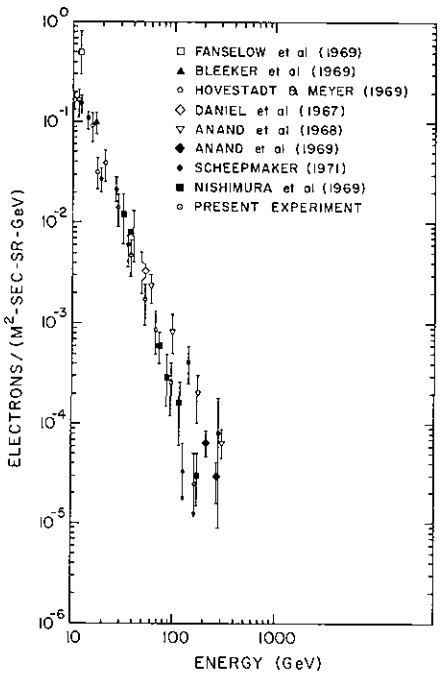

7. Conclusions

While the intensity in figure 5 agrees with the results of others at about 10 GeV, the spectrum is significantly steeper. The data can be fitted to a power law with a spectral index of -3.1 $\pm$0.2.

Our measured spectrum shows no sharp break but a consistent dropoff of the intensity of primary cosmic ray electrons. The spectral index of -3.1 may indicate a spectrum steepened by 0.5 power from -2.6. If the spectrum at lower energies has an index of -2.6, then steepening by half a power may occur in range of 10 GeV or below. This would be consistent with the model suggested by Jokipii and Meyer (1968) in which cosmic ray electrons diffuse in an isotropic medium.

8. References

Anand, K.C., Daniel, R.R., Stephens, S.A., 1968, Phys. Rev. Letters 20, 764.

Anand, K.C., Daniel, R.R., Stephens, S.A., 1969, Paper OG-11, 11th Int. Conf. on Cosmic Rays, Budapest.

Bleeker, J.A.M., Burger, J.J., Deerenberg, A.J.M., Hulst, H.C., Scheepmaker, A., Swanenburg, B.N., Tanaka, Y., 1969, paper OG-34, 11th Int. Conf. on Cosmic Rays, Budapest.

Daniel, R.R., Stephens, S.A., 1969, Proc. Ind. Acad. Sci., 65, 319.

Fanselow, J.L., Hartman, R.C., Hildebrand, R.H., Meyer, P., 1969, Ap. J. 158, 771.

Hovestadt, D., Meyer, P., 1969, paper MO-118, 11th Int. Conf. on Cosmic Rays, Budapest.

Jokipii, J.R. and Meyer, P., 1968, Phys. Rev. Letters 20, 752.
Nishimura, J., Mikumo, E., Mito, I., Niu, K., Ohta, I., Tiara, T., 1969, paper OG-43, 11th Int. Conf. on Cosmic Rays, Budapest.
Ryan, M.J., Ormes, J.F., Balasubrahmanyan, V.K., 1971, "The Cosmic Ray Proton and Helium Spectra above 50 GeV", this conference.
Scheepmaker, A., "Primary Cosmic Ray Electron Spectrum between 5 and $\simeq$ 300 GeV", unpublished, University of Leiden, 1971.